

Study of two-photon decays of pseudoscalar mesons
via J/ψ radiative decays

M. Ablikim¹, M. N. Achasov^{9,d}, S. Ahmed¹⁴, M. Albrecht⁴, A. Amoroso^{53A,53C}, F. F. An¹, Q. An^{50,40}, J. Z. Bai¹, Y. Bai³⁹, O. Bakina²⁴, R. Baldini Ferroli^{20A}, Y. Ban³², D. W. Bennett¹⁹, J. V. Bennett⁵, N. Berger²³, M. Bertani^{20A}, D. Bettoni^{21A}, J. M. Bian⁴⁷, F. Bianchi^{53A,53C}, E. Boger^{24,b}, I. Boyko²⁴, R. A. Briere⁵, H. Cai⁵⁵, X. Cai^{1,40}, O. Cakir^{43A}, A. Calcaterra^{20A}, G. F. Cao^{1,44}, S. A. Cetin^{43B}, J. Chai^{53C}, J. F. Chang^{1,40}, G. Chelkov^{24,b,c}, G. Chen¹, H. S. Chen^{1,44}, J. C. Chen¹, M. L. Chen^{1,40}, P. L. Chen⁵¹, S. J. Chen³⁰, X. R. Chen²⁷, Y. B. Chen^{1,40}, X. K. Chu³², G. Cibinetto^{21A}, H. L. Dai^{1,40}, J. P. Dai^{35,h}, A. Dbeyssi¹⁴, D. Dedovich²⁴, Z. Y. Deng¹, A. Denig²³, I. Denysenko²⁴, M. Destefanis^{53A,53C}, F. De Mori^{53A,53C}, Y. Ding²⁸, C. Dong³¹, J. Dong^{1,40}, L. Y. Dong^{1,44}, M. Y. Dong^{1,40,44}, Z. L. Dou³⁰, S. X. Du⁵⁷, P. F. Duan¹, J. Fang^{1,40}, S. S. Fang^{1,44}, Y. Fang¹, R. Farinelli^{21A,21B}, L. Fava^{53B,53C}, S. Fegan²³, F. Feldbauer²³, G. Felici^{20A}, C. Q. Feng^{50,40}, E. Fioravanti^{21A}, M. Fritsch^{23,14}, C. D. Fu¹, Q. Gao¹, X. L. Gao^{50,40}, Y. Gao⁴², Y. G. Gao⁶, Z. Gao^{50,40}, I. Garzia^{21A}, K. Goetzen¹⁰, L. Gong³¹, W. X. Gong^{1,40}, W. Gradl²³, M. Greco^{53A,53C}, M. H. Gu^{1,40}, Y. T. Gu¹², A. Q. Guo¹, R. P. Guo^{1,44}, Y. P. Guo²³, Z. Haddadi²⁶, S. Han⁵⁵, X. Q. Hao¹⁵, F. A. Harris⁴⁵, K. L. He^{1,44}, X. Q. He⁴⁹, F. H. Heinsius⁴, T. Held⁴, Y. K. Heng^{1,40,44}, T. Holtmann⁴, Z. L. Hou¹, H. M. Hu^{1,44}, T. Hu^{1,40,44}, Y. Hu¹, G. S. Huang^{50,40}, J. S. Huang¹⁵, X. T. Huang³⁴, X. Z. Huang³⁰, Z. L. Huang²⁸, T. Hussain⁵², W. Ikegami Andersson⁵⁴, Q. Ji¹, Q. P. Ji¹⁵, X. B. Ji^{1,44}, X. L. Ji^{1,40}, X. S. Jiang^{1,40,44}, X. Y. Jiang³¹, J. B. Jiao³⁴, Z. Jiao¹⁷, D. P. Jin^{1,40,44}, S. Jin^{1,44}, Y. Jin⁴⁶, T. Johansson⁵⁴, A. Julin⁴⁷, N. Kalantar-Nayestanaki²⁶, X. L. Kang¹, X. S. Kang³¹, M. Kavatsyuk²⁶, B. C. Ke⁵, T. Khan^{50,40}, A. Khoukaz⁴⁸, P. Kiese²³, R. Kliemt¹⁰, L. Koch²⁵, O. B. Kolcu^{43B,f}, B. Kopf⁴, M. Kornicer⁴⁵, M. Kuemmel⁴, M. Kuhlmann⁴, A. Kupsc⁵⁴, W. Kühn²⁵, J. S. Lange²⁵, M. Lara¹⁹, P. Larin¹⁴, L. Lavezzi^{53C}, H. Leithoff²³, C. Leng^{53C}, C. Li⁵⁴, Cheng Li^{50,40}, D. M. Li⁵⁷, F. Li^{1,40}, F. Y. Li³², G. Li¹, H. B. Li^{1,44}, H. J. Li^{1,44}, J. C. Li¹, Jin Li³³, K. J. Li⁴¹, Kang Li¹³, Ke Li³⁴, Lei Li³, P. L. Li^{50,40}, P. R. Li^{44,7}, Q. Y. Li³⁴, W. D. Li^{1,44}, W. G. Li¹, X. L. Li³⁴, X. N. Li^{1,40}, X. Q. Li³¹, Z. B. Li⁴¹, H. Liang^{50,40}, Y. F. Liang³⁷, Y. T. Liang²⁵, G. R. Liao¹¹, D. X. Lin¹⁴, B. Liu^{35,h}, B. J. Liu¹, C. X. Liu¹, D. Liu^{50,40}, F. H. Liu³⁶, Fang Liu¹, Feng Liu⁶, H. B. Liu¹², H. M. Liu^{1,44}, Huanhuan Liu¹, Huihui Liu¹⁶, J. B. Liu^{50,40}, J. P. Liu⁵⁵, J. Y. Liu^{1,44}, K. Liu⁴², K. Y. Liu²⁸, Ke Liu⁶, L. D. Liu³², P. L. Liu^{1,40}, Q. Liu⁴⁴, S. B. Liu^{50,40}, X. Liu²⁷, Y. B. Liu³¹, Z. A. Liu^{1,40,44}, Zhiqing Liu²³, Y. F. Long³², X. C. Lou^{1,40,44}, H. J. Lu¹⁷, J. G. Lu^{1,40}, Y. Lu¹, Y. P. Lu^{1,40}, C. L. Luo²⁹, M. X. Luo⁵⁶, T. Luo⁴⁵, X. L. Luo^{1,40}, X. R. Lyu⁴⁴, F. C. Ma²⁸, H. L. Ma¹, L. L. Ma³⁴, M. M. Ma^{1,44}, Q. M. Ma¹, T. Ma¹, X. N. Ma³¹, X. Y. Ma^{1,40}, Y. M. Ma³⁴, F. E. Maas¹⁴, M. Maggiora^{53A,53C}, Q. A. Malik⁵², Y. J. Mao³², Z. P. Mao¹, S. Marcello^{53A,53C}, Z. X. Meng⁴⁶, J. G. Messchendorp²⁶, G. Mezzadri^{21B}, J. Min^{1,40}, T. J. Min¹, R. E. Mitchell¹⁹, X. H. Mo^{1,40,44}, Y. J. Mo⁶, C. Morales Morales¹⁴, N. Yu. Muchnoi^{9,d}, H. Muramatsu⁴⁷, P. Musiol⁴, A. Mustafa⁴, Y. Nefedov²⁴, F. Nerling¹⁰, I. B. Nikolaev^{9,d}, Z. Ning^{1,40}, S. Nisar⁸, S. L. Niu^{1,40}, X. Y. Niu^{1,44}, S. L. Olsen^{33,j}, Q. Ouyang^{1,40,44}, S. Pacetti^{20B}, Y. Pan^{50,40}, M. Papenbrock⁵⁴, P. Patteri^{20A}, M. Pelizaeus⁴, J. Pellegrino^{53A,53C}, H. P. Peng^{50,40}, K. Peters^{10,g}, J. Pettersson⁵⁴, J. L. Ping²⁹, R. G. Ping^{1,44}, R. Poling⁴⁷, V. Prasad^{50,40}, H. R. Qi², M. Qi³⁰, S. Qian^{1,40}, C. F. Qiao⁴⁴, J. J. Qin⁴⁴, N. Qin⁵⁵, X. S. Qin⁴, Z. H. Qin^{1,40}, J. F. Qiu¹, K. H. Rashid^{52,i}, C. F. Redmer²³, M. Richter⁴, M. Ripka²³, G. Rong^{1,44}, Ch. Rosner¹⁴, A. Sarantsev^{24,e}, M. Savrié^{21B}, C. Schnier⁴, K. Schoenning⁵⁴, W. Shan³², M. Shao^{50,40}, C. P. Shen², P. X. Shen³¹, X. Y. Shen^{1,44}, H. Y. Sheng¹, J. J. Song³⁴, W. M. Song³⁴, X. Y. Song¹, S. Sosio^{53A,53C}, C. Sowa⁴, S. Spataro^{53A,53C}, G. X. Sun¹, J. F. Sun¹⁵, L. Sun⁵⁵, S. S. Sun^{1,44}, X. H. Sun¹, Y. J. Sun^{50,40}, Y. K. Sun^{50,40}, Y. Z. Sun¹, Z. J. Sun^{1,40}, Z. T. Sun¹⁹, C. J. Tang³⁷, G. Y. Tang¹, X. Tang¹, I. Tapan^{43C}, M. Tiemens²⁶, B. Tsednee²², I. Uman^{43D}, G. S. Varner⁴⁵, B. Wang¹, B. L. Wang⁴⁴, D. Wang³², D. Y. Wang³², Dan Wang⁴⁴, K. Wang^{1,40}, L. L. Wang¹, L. S. Wang¹, M. Wang³⁴, Meng Wang^{1,44}, P. Wang¹, P. L. Wang¹, W. P. Wang^{50,40}, X. F. Wang⁴², Y. Wang³⁸, Y. D. Wang¹⁴, Y. F. Wang^{1,40,44}, Y. Q. Wang²³, Z. Wang^{1,40}, Z. G. Wang^{1,40}, Z. Y. Wang¹, Zongyuan Wang^{1,44}, T. Weber²³, D. H. Wei¹¹, P. Weidenkaff²³, S. P. Wen¹, U. Wiedner⁴, M. Wolke⁵⁴, L. H. Wu¹, L. J. Wu^{1,44}, Z. Wu^{1,40}, L. Xia^{50,40}, Y. Xia¹⁸, D. Xiao¹, H. Xiao⁵¹, Y. J. Xiao^{1,44}, Z. J. Xiao²⁹, Y. G. Xie^{1,40}, Y. H. Xie⁶, X. A. Xiong^{1,44}, Q. L. Xiu^{1,40}, G. F. Xu¹, J. J. Xu^{1,44}, L. Xu¹, Q. J. Xu¹³, Q. N. Xu⁴⁴, X. P. Xu³⁸, L. Yan^{53A,53C}, W. B. Yan^{50,40}, Y. H. Yan¹⁸, H. J. Yang^{35,h}, H. X. Yang¹, L. Yang⁵⁵, Y. H. Yang³⁰, Y. X. Yang¹¹, M. Ye^{1,40}, M. H. Ye⁷, J. H. Yin¹, Z. Y. You⁴¹, B. X. Yu^{1,40,44}, C. X. Yu³¹, J. S. Yu²⁷, C. Z. Yuan^{1,44}, Y. Yuan¹, A. Yuncu^{43B,a}, A. A. Zafar⁵², Y. Zeng¹⁸, Z. Zeng^{50,40}, B. X. Zhang¹, B. Y. Zhang^{1,40}, C. C. Zhang¹, D. H. Zhang¹, H. H. Zhang⁴¹, H. Y. Zhang^{1,40}, J. Zhang^{1,44}, J. L. Zhang¹, J. Q. Zhang¹, J. W. Zhang^{1,40,44}, J. Y. Zhang¹, J. Z. Zhang^{1,44}, K. Zhang^{1,44}, L. Zhang⁴², S. Q. Zhang³¹, X. Y. Zhang³⁴, Y. H. Zhang^{1,40}, Y. T. Zhang^{50,40}, Yang Zhang¹, Yao Zhang¹, Yu Zhang⁴⁴, Z. H. Zhang⁶,

Z. P. Zhang⁵⁰, Z. Y. Zhang⁵⁵, G. Zhao¹, J. W. Zhao^{1,40}, J. Y. Zhao^{1,44}, J. Z. Zhao^{1,40}, Lei Zhao^{50,40}, Ling Zhao¹, M. G. Zhao³¹, Q. Zhao¹, S. J. Zhao⁵⁷, T. C. Zhao¹, Y. B. Zhao^{1,40}, Z. G. Zhao^{50,40}, A. Zhemchugov^{24,b}, B. Zheng⁵¹, J. P. Zheng^{1,40}, Y. H. Zheng⁴⁴, B. Zhong²⁹, L. Zhou^{1,40}, X. Zhou⁵⁵, X. K. Zhou^{50,40}, X. R. Zhou^{50,40}, X. Y. Zhou¹, Y. X. Zhou¹², J. Zhu³¹, J. Zhu⁴¹, K. Zhu¹, K. J. Zhu^{1,40,44}, S. Zhu¹, S. H. Zhu⁴⁹, X. L. Zhu⁴², Y. C. Zhu^{50,40}, Y. S. Zhu^{1,44}, Z. A. Zhu^{1,44}, J. Zhuang^{1,40}, L. Zotti^{53A,53C}, B. S. Zou¹, J. H. Zou¹

(BESIII Collaboration)

¹ *Institute of High Energy Physics, Beijing 100049, People's Republic of China*

² *Beihang University, Beijing 100191, People's Republic of China*

³ *Beijing Institute of Petrochemical Technology, Beijing 102617, People's Republic of China*

⁴ *Bochum Ruhr-University, D-44780 Bochum, Germany*

⁵ *Carnegie Mellon University, Pittsburgh, Pennsylvania 15213, USA*

⁶ *Central China Normal University, Wuhan 430079, People's Republic of China*

⁷ *China Center of Advanced Science and Technology, Beijing 100190, People's Republic of China*

⁸ *COMSATS Institute of Information Technology, Lahore, Defence Road, Off Raiwind Road, 54000 Lahore, Pakistan*

⁹ *G.I. Budker Institute of Nuclear Physics SB RAS (BINP), Novosibirsk 630090, Russia*

¹⁰ *GSI Helmholtzcentre for Heavy Ion Research GmbH, D-64291 Darmstadt, Germany*

¹¹ *Guangxi Normal University, Guilin 541004, People's Republic of China*

¹² *Guangxi University, Nanning 530004, People's Republic of China*

¹³ *Hangzhou Normal University, Hangzhou 310036, People's Republic of China*

¹⁴ *Helmholtz Institute Mainz, Johann-Joachim-Becher-Weg 45, D-55099 Mainz, Germany*

¹⁵ *Henan Normal University, Xinxiang 453007, People's Republic of China*

¹⁶ *Henan University of Science and Technology, Luoyang 471003, People's Republic of China*

¹⁷ *Huangshan College, Huangshan 245000, People's Republic of China*

¹⁸ *Hunan University, Changsha 410082, People's Republic of China*

¹⁹ *Indiana University, Bloomington, Indiana 47405, USA*

²⁰ *(A)INFN Laboratori Nazionali di Frascati, I-00044, Frascati,*

Italy; (B)INFN and University of Perugia, I-06100, Perugia, Italy

²¹ *(A)INFN Sezione di Ferrara, I-44122, Ferrara, Italy; (B)University of Ferrara, I-44122, Ferrara, Italy*

²² *Institute of Physics and Technology, Peace Ave. 54B, Ulaanbaatar 13330, Mongolia*

²³ *Johannes Gutenberg University of Mainz, Johann-Joachim-Becher-Weg 45, D-55099 Mainz, Germany*

²⁴ *Joint Institute for Nuclear Research, 141980 Dubna, Moscow region, Russia*

²⁵ *Justus-Liebig-Universitaet Giessen, II. Physikalisches Institut, Heinrich-Buff-Ring 16, D-35392 Giessen, Germany*

²⁶ *KVI-CART, University of Groningen, NL-9747 AA Groningen, The Netherlands*

²⁷ *Lanzhou University, Lanzhou 730000, People's Republic of China*

²⁸ *Liaoning University, Shenyang 110036, People's Republic of China*

²⁹ *Nanjing Normal University, Nanjing 210023, People's Republic of China*

³⁰ *Nanjing University, Nanjing 210093, People's Republic of China*

³¹ *Nankai University, Tianjin 300071, People's Republic of China*

³² *Peking University, Beijing 100871, People's Republic of China*

³³ *Seoul National University, Seoul, 151-747 Korea*

³⁴ *Shandong University, Jinan 250100, People's Republic of China*

³⁵ *Shanghai Jiao Tong University, Shanghai 200240, People's Republic of China*

³⁶ *Shanxi University, Taiyuan 030006, People's Republic of China*

³⁷ *Sichuan University, Chengdu 610064, People's Republic of China*

³⁸ *Soochow University, Suzhou 215006, People's Republic of China*

³⁹ *Southeast University, Nanjing 211100, People's Republic of China*

⁴⁰ *State Key Laboratory of Particle Detection and Electronics,*

Beijing 100049, Hefei 230026, People's Republic of China

⁴¹ *Sun Yat-Sen University, Guangzhou 510275, People's Republic of China*

⁴² *Tsinghua University, Beijing 100084, People's Republic of China*

⁴³ *(A)Ankara University, 06100 Tandogan, Ankara, Turkey; (B)Istanbul Bilgi*

University, 34060 Eyup, Istanbul, Turkey; (C)Uludag University, 16059 Bursa,

Turkey; (D)Near East University, Nicosia, North Cyprus, Mersin 10, Turkey

- ⁴⁴ *University of Chinese Academy of Sciences, Beijing 100049, People's Republic of China*
⁴⁵ *University of Hawaii, Honolulu, Hawaii 96822, USA*
⁴⁶ *University of Jinan, Jinan 250022, People's Republic of China*
⁴⁷ *University of Minnesota, Minneapolis, Minnesota 55455, USA*
⁴⁸ *University of Muenster, Wilhelm-Klemm-Str. 9, 48149 Muenster, Germany*
⁴⁹ *University of Science and Technology Liaoning, Anshan 114051, People's Republic of China*
⁵⁰ *University of Science and Technology of China, Hefei 230026, People's Republic of China*
⁵¹ *University of South China, Hengyang 421001, People's Republic of China*
⁵² *University of the Punjab, Lahore-54590, Pakistan*
⁵³ (A)*University of Turin, I-10125, Turin, Italy; (B)University of Eastern Piedmont, I-15121, Alessandria, Italy; (C)INFN, I-10125, Turin, Italy*
⁵⁴ *Uppsala University, Box 516, SE-75120 Uppsala, Sweden*
⁵⁵ *Wuhan University, Wuhan 430072, People's Republic of China*
⁵⁶ *Zhejiang University, Hangzhou 310027, People's Republic of China*
⁵⁷ *Zhengzhou University, Zhengzhou 450001, People's Republic of China*
- ^a *Also at Bogazici University, 34342 Istanbul, Turkey*
^b *Also at the Moscow Institute of Physics and Technology, Moscow 141700, Russia*
^c *Also at the Functional Electronics Laboratory, Tomsk State University, Tomsk, 634050, Russia*
^d *Also at the Novosibirsk State University, Novosibirsk, 630090, Russia*
^e *Also at the NRC "Kurchatov Institute", PNPI, 188300, Gatchina, Russia*
^f *Also at Istanbul Arel University, 34295 Istanbul, Turkey*
^g *Also at Goethe University Frankfurt, 60323 Frankfurt am Main, Germany*
^h *Also at Key Laboratory for Particle Physics, Astrophysics and Cosmology, Ministry of Education; Shanghai Key Laboratory for Particle Physics and Cosmology; Institute of Nuclear and Particle Physics, Shanghai 200240, People's Republic of China*
ⁱ *Government College Women University, Sialkot - 51310. Punjab, Pakistan.*
^j *Currently at: Center for Underground Physics, Institute for Basic Science, Daejeon 34126, Korea*
(Dated: November 16, 2021)

Using a sample of 4.48×10^8 $\psi(3686)$ events collected with the BESIII detector at the BEPCII collider, we study the two-photon decays of the pseudoscalar mesons π^0 , η , η' , $\eta(1405)$, $\eta(1475)$, $\eta(1760)$, and $X(1835)$ in J/ψ radiative decays using $\psi(3686) \rightarrow \pi^+\pi^- J/\psi$ events. The π^0 , η and η' mesons are clearly observed in the two-photon mass spectra, and the branching fractions are determined to be $B(J/\psi \rightarrow \gamma\pi^0 \rightarrow 3\gamma) = (3.57 \pm 0.12 \pm 0.16) \times 10^{-5}$, $B(J/\psi \rightarrow \gamma\eta \rightarrow 3\gamma) = (4.42 \pm 0.04 \pm 0.18) \times 10^{-4}$, and $B(J/\psi \rightarrow \gamma\eta' \rightarrow 3\gamma) = (1.26 \pm 0.02 \pm 0.05) \times 10^{-4}$, where the first errors are statistical and the second systematic. No clear signal for $\eta(1405)$, $\eta(1475)$, $\eta(1760)$ or $X(1835)$ is observed in the two-photon mass spectra, and upper limits at the 90% confidence level on the product branching fractions are obtained.

PACS numbers: 13.66.Bc, 14.40.Be

I. INTRODUCTION

Within the framework of quantum chromodynamics (QCD), the two-photon decay width of a meson plays a crucial role in understanding the nature of the meson and helps to distinguish glueballs from conventional mesons since glueballs are believed to have a relatively small two-photon decay width [1]. Therefore, experimental studies of the two-photon decays of mesons are very important to help interpret the meson spectrum.

The $\eta(1405)/\eta(1475)$ pseudoscalar meson was once regarded as a glueball candidate since it was copiously produced in J/ψ radiative decays [2] and was not observed in two-photon collisions [3]. However, the measured mass is much lower than the prediction of Lattice QCD for a

pseudoscalar glueball, which lies above $2\text{GeV}/c^2$ [4, 5]. Later, the experiments found two different pseudoscalar states, $\eta(1405)$ and $\eta(1475)$, with the former mainly decaying to $a_0(980)\pi$ and $K\bar{K}\pi$ and the latter mainly to $K^*(892)\bar{K}$ [6]. At present, the one state assumption and the nature of $\eta(1405)/\eta(1475)$ are still controversial. Another pseudoscalar meson, the $\eta(1760)$, has been proposed as a mixture of a glueball with a conventional $q\bar{q}$ state [7], rather than a pure $q\bar{q}$ meson or a glueball, and this hypothesis is supported by the large production rate of the $\eta(1760)$ in $J/\psi \rightarrow \gamma\omega\omega$ decays [8, 9]. The nature of the $X(1835)$ is still an open question although a number of theoretical interpretations have been proposed, including an $N\bar{N}$ bound state [10], baryonium with sizable gluon content [11], a pseudoscalar glueball [12], a radial

excitation of the η' [13], and an η_c -glueball mixture [14]. None of these interpretations have been completely ruled out or confirmed.

Pseudoscalar mesons are copiously produced in J/ψ radiative decays. The two-photon decay widths of π^0 , η and η' mesons have been measured [6], and previous values were used to determine the branching fractions of $J/\psi \rightarrow \gamma(\pi^0, \eta, \eta')$ [15, 16]. Those of $J/\psi \rightarrow \gamma(\eta, \eta')$ were then used to calculate the pseudoscalar mixing angle [15]. However, the two-photon decays of $\eta(1405)$, $\eta(1475)$, $\eta(1760)$ and $X(1835)$ have not been investigated yet.

At present, the sample of 4.48×10^8 $\psi(3686)$ events [17] (1.06×10^8 events in 2009 and 3.41×10^8 in 2012) collected by the BESIII detector offers the opportunity to study the two-photon decays of pseudoscalar mesons in J/ψ radiative decay in $\psi(3686) \rightarrow \pi^+\pi^-J/\psi$ events. While the number of J/ψ events from the BESIII $\psi(3686) \rightarrow \pi^+\pi^-J/\psi$ data samples is much smaller than that of the direct BESIII $e^+e^- \rightarrow J/\psi$ samples, the direct J/ψ samples have a large background from the $e^+e^- \rightarrow \gamma\gamma$ process. Thus, better sensitivity on the two-photon decay widths of pseudoscalar mesons is possible using the $\psi(3686)$ data samples collected at BESIII. In this paper, the branching fractions of $J/\psi \rightarrow \gamma(\pi^0, \eta, \eta') \rightarrow 3\gamma$ are measured. Additionally, we also search for the two-photon decays of the pseudoscalar mesons, $\eta(1405)$, $\eta(1475)$, $\eta(1760)$ and $X(1835)$.

II. DETECTOR AND MONTE CARLO SIMULATION

BEPCII is a double-ring e^+e^- collider running at center-of-mass energies from 2.0 to 4.6 GeV. The BESIII [18] detector at BEPCII, with a geometrical acceptance of 93% of 4π solid angle, operates in a 1.0 T magnetic field provided by a superconducting solenoid magnet. The detector is composed of a helium-based drift chamber (MDC), a plastic-scintillator time-of-flight (TOF) system, a CsI(Tl) electromagnetic calorimeter (EMC) and a resistive plate chamber (RPC)-based muon chamber (MUC) in the iron flux return yoke of the magnet. The spatial resolution of the MDC is better than 130 μm , the charged-particle momentum resolution is 0.5% at 1.0 GeV/c, and the specific energy loss (dE/dx) resolution is better than 6% for electrons from Bhabha events. The time resolution of the TOF is 80 ps in the barrel and 110 ps in the endcaps. The energy resolution of the EMC at 1.0 GeV/c is 2.5% (5%) in the barrel (endcaps), and the position resolution is better than 6 mm (9 mm) in the barrel (endcaps). The position resolution in the MUC is better than 2 cm.

Monte Carlo (MC) simulations are used to estimate backgrounds and determine the detection efficiencies. The GEANT4-based [19] simulation software BOOST [20] includes the geometric and material description of the BESIII detector, detector response, and

digitization models, as well as the tracking of the detector running conditions and performance. Production of the charmonium state $\psi(3686)$ is simulated with KKMC [21, 22], while the decays are generated with EVTGEN [23, 24] for known decay modes with branching fractions taken from the Particle Data Group (PDG) [6] and by LUNDCHARM [25] for the remaining unknown decays. We use a sample of 5.06×10^8 simulated $\psi(3686)$ events, in which the $\psi(3686)$ decays generically ('inclusive MC sample'), to study the backgrounds. The analysis is performed in the framework of the BESIII offline software system (BOSS) [26] which incorporates the detector calibration, event reconstruction, and data storage.

III. DATA ANALYSIS

In this paper, the two-photon decays of the pseudoscalar mesons are investigated with J/ψ radiative decays. Hence the candidate events for the reconstruction of $\psi(3686) \rightarrow \pi^+\pi^-J/\psi$, $J/\psi \rightarrow 3\gamma$ are required to have two oppositely charged tracks and at least three photon candidates. Each charged track, reconstructed using hits in the MDC, is required to be in the polar angle range $|\cos\theta| < 0.93$ and pass the interaction point within ± 10 cm along the beam direction, and within ± 1 cm in the plane perpendicular to the beam. Both charged tracks are assumed to be pion candidates.

Photon candidates are reconstructed from clusters of energy deposited in the EMC, and the deposited energy of each is required to be larger than 25 MeV in the barrel region ($|\cos\theta| < 0.80$) or 50 MeV in the endcap region ($0.86 < |\cos\theta| < 0.92$). The opening angle between a shower and the nearest charged track must be greater than 15° , and timing requirements in the EMC are used to suppress electronic noise and energy deposits unrelated with the collision event. Events that satisfy the above requirements are retained for further analysis.

A four-constraint (4C) kinematic fit imposing energy and momentum conservation is performed under the hypothesis of $\pi^+\pi^-\gamma\gamma\gamma$. If the number of photon candidates in an event is larger than three, the combination with the smallest χ_{4C}^2 from the kinematic fit is selected, and χ_{4C}^2 is further required to be less than 50. The distribution of the $\gamma\gamma\gamma$ invariant mass, $M_{\gamma\gamma\gamma}$, of selected candidate events is shown in Fig. 1, where a very clean J/ψ peak is seen with very low background. A mass window requirement $|M_{\gamma\gamma\gamma} - m_{J/\psi}| < 0.08 \text{ GeV}/c^2$ is applied to select the J/ψ signal, where $m_{J/\psi}$ is the nominal mass of the J/ψ meson [6].

After the above requirements, the distribution of the two-photon invariant mass $M_{\gamma\gamma}$ is shown in Fig. 2, where the photon momenta from the 4C kinematic fit are used to calculate $M_{\gamma\gamma}$ and there are three entries per event.

The backgrounds without the J/ψ intermediate state (non- J/ψ background) can be estimated from the events within the J/ψ sideband regions, defined

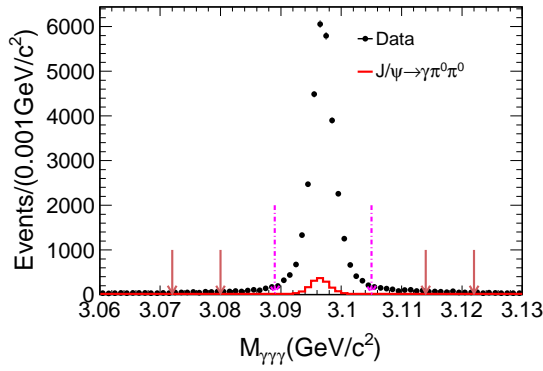


FIG. 1. (color online) Three-photon invariant mass spectrum $M_{\gamma\gamma}$ for data (dots with error bars) and MC simulation of the background contribution from $J/\psi \rightarrow \gamma\pi^0\pi^0$ (red solid histogram). The pink dot-dashed arrows indicate the signal region for selection of J/ψ events, and the brown solid arrows show the sideband regions.

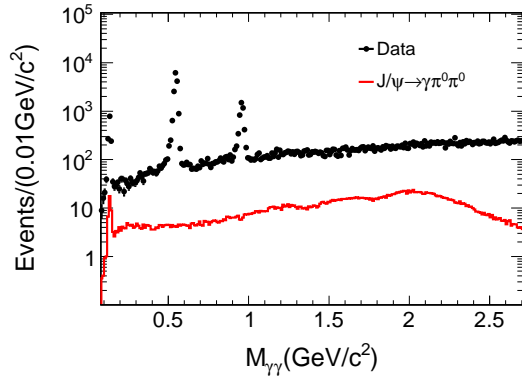


FIG. 2. (color online) Two-photon invariant mass spectrum for data (dots with error bars) and MC simulation of $J/\psi \rightarrow \gamma\pi^0\pi^0$ (red solid histogram).

as $3.072 \text{ GeV}/c^2 < M_{\gamma\gamma} < 3.080 \text{ GeV}/c^2$ and $3.114 \text{ GeV}/c^2 < M_{\gamma\gamma} < 3.122 \text{ GeV}/c^2$, which are indicated in Fig. 1. The backgrounds from $\psi(3686) \rightarrow \pi^+\pi^-J/\psi$ with J/ψ decaying to neutral particle final states (J/ψ background) are investigated with the inclusive MC sample of $5.06 \times 10^8 \psi(3686)$ events. One prominent background is $\psi(3686) \rightarrow \pi^+\pi^-J/\psi$, with $J/\psi \rightarrow \gamma\pi^0\pi^0$, which produces a peak around the π^0 mass region in the $M_{\gamma\gamma}$ distribution. To estimate its contribution, a dedicated MC sample of $\psi(3686) \rightarrow \pi^+\pi^-J/\psi$, $J/\psi \rightarrow \gamma\pi^0\pi^0$ is produced incorporating the amplitude analysis result of $J/\psi \rightarrow \gamma\pi^0\pi^0$ [27]. With the same selection criteria and taking into account the number of $\psi(3686)$ events as well as the branching fractions of $\psi(3686) \rightarrow \pi^+\pi^-J/\psi$ [6] and $J/\psi \rightarrow \gamma\pi^0\pi^0$ [27], the corresponding distribution of $M_{\gamma\gamma}$ is shown as the solid histogram in Fig. 2. The number of peaking background events in the π^0 signal region is expected to be 32 ± 2 , which is estimated by a fit to the $\gamma\gamma$ invariant mass spectrum of the above MC sample, where the π^0 signal is

modeled with the sum of a Crystal Ball (CB) [28] function and a Gaussian function, and the other J/ψ non-peaking background is described with a second order Chebychev polynomial function.

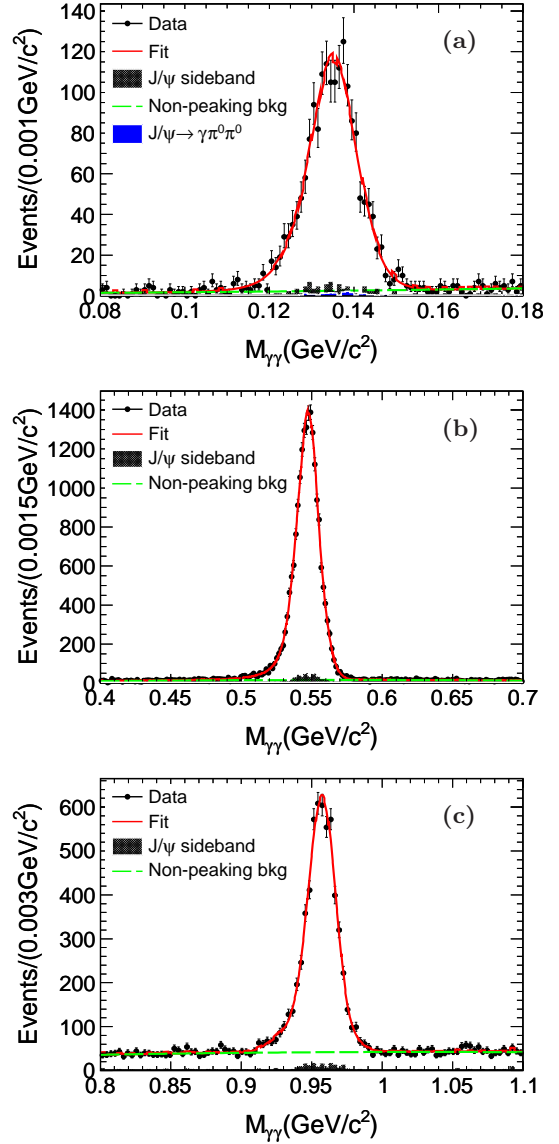


FIG. 3. (color online) Fits to the $\gamma\gamma$ mass distribution for (a) $J/\psi \rightarrow \gamma\pi^0 \rightarrow 3\gamma$, (b) $J/\psi \rightarrow \gamma\eta \rightarrow 3\gamma$ and (c) $J/\psi \rightarrow \gamma\eta' \rightarrow 3\gamma$. The dots with error bars are data; the red solid curve is the result of the fit; the black hatched histogram shows the J/ψ sideband background; the long-dashed curve represents the other non-peaking backgrounds; the blue solid histogram in (a) represents the contribution from the background of $J/\psi \rightarrow \gamma\pi^0\pi^0$.

The signal yields of $J/\psi \rightarrow \gamma(\pi^0, \eta, \eta') \rightarrow 3\gamma$ are obtained from unbinned maximum likelihood fits to the $\gamma\gamma$ invariant mass spectra. In the fits, the signal shapes are modeled with the sum of a CB function and a Gaussian function. The non- J/ψ backgrounds are estimated with the events in the J/ψ sideband region, assuming the

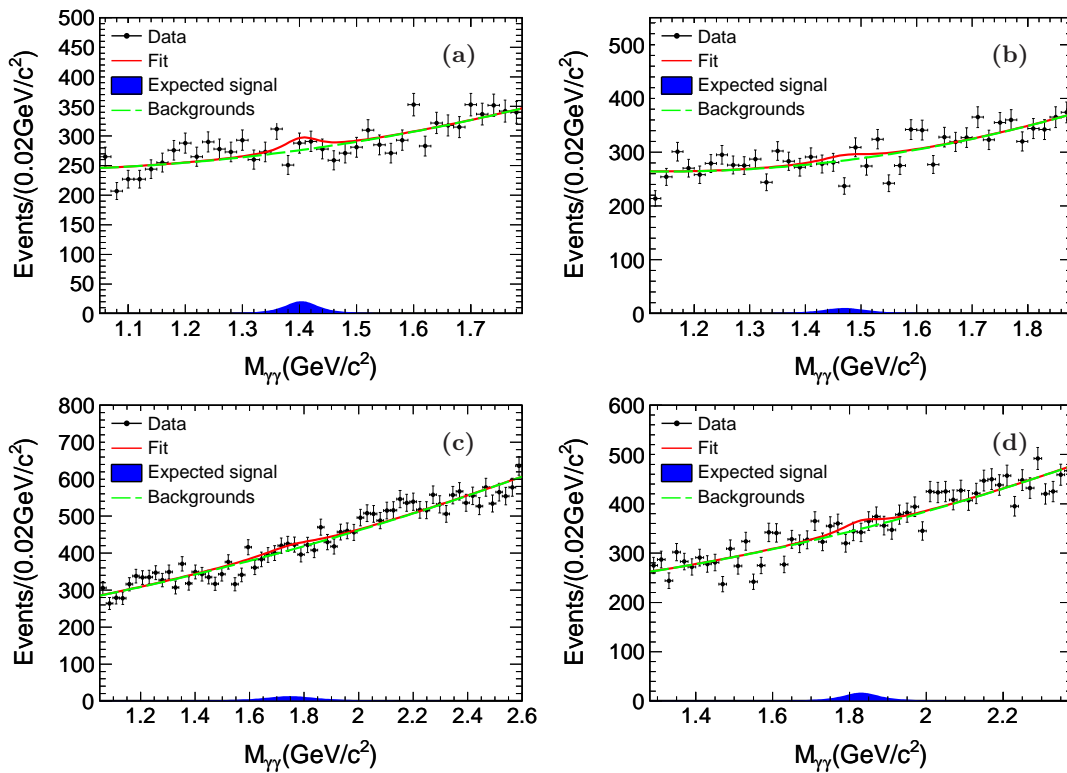


FIG. 4. (color online) Fit results for the $\gamma\gamma$ invariant mass distributions for (a) $J/\psi \rightarrow \gamma\eta(1405) \rightarrow 3\gamma$, (b) $J/\psi \rightarrow \gamma\eta(1475) \rightarrow 3\gamma$, (c) $J/\psi \rightarrow \gamma\eta(1760) \rightarrow 3\gamma$ and (d) $J/\psi \rightarrow \gamma X(1835) \rightarrow 3\gamma$. The dots with error bars are data, the red solid curves show the result of the fit, the blue shaded histograms are the expected signals, where the signal normalization corresponds to the 90% confidence level upper limit, and the green long-dashed curves show the background.

$M_{\gamma\gamma}$ distribution to be flat in the vicinity of the J/ψ . Their yields and shapes are fixed in the fit. The non-peaking J/ψ background is parameterized with a second-order Chebychev polynomial function. The fit results are shown in Fig. 3. The signal yields from the fit and the MC determined detection efficiencies are summarized in Table I, where the MC simulation is performed using an angular distribution of $1 + \cos^2 \theta_\gamma$ for the radiative photon in the J/ψ rest frame.

No obvious signals for the pseudoscalar mesons $\eta(1405)$, $\eta(1475)$, $\eta(1760)$ or $X(1835)$ are observed in the $M_{\gamma\gamma}$ distributions. Upper limits on the signal yields are obtained by fits to the $M_{\gamma\gamma}$ distributions in the vicinity of the corresponding signal region, as shown in Fig. 4. In the fits, the line shapes of the $\eta(1405)$, $\eta(1475)$, $\eta(1760)$ and $X(1835)$ signals are parameterized by Breit Wigner (BW) functions convolved with Gaussian functions to account for the mass resolution, where the mass and width of BW functions are fixed to the world average values taken from the PDG [6] and the mass resolutions are obtained from MC simulation. The background shapes are described by second-order Chebychev polynomial functions. We derive the upper limits from these fits using a Bayesian approach with a flat prior as input. The distribution of minimized likelihood values for a series of input signal event yields is taken as the probability den-

sity function (PDF) for the expected number of events. The number of events at 90% of the integral of the PDF from 0 to the given number of events is defined as the upper limit at the 90% confidence level (C.L.). To take into account the systematic uncertainties related to the fits, alternative fits with different fit ranges and background shapes are also performed, and the maximum upper limit among these cases is selected.

IV. SYSTEMATIC UNCERTAINTIES

Systematic uncertainties in the branching fraction measurements mainly originate from efficiency differences between data and MC simulation in the MDC tracking, the photon detection, the kinematic fitting efficiency and the J/ψ mass window requirement. Additional uncertainties associated with the fit range, the background shape, the sideband regions, the MC statistics, the branching fraction of $\psi(3686) \rightarrow \pi^+\pi^- J/\psi$, and the total number of $\psi(3686)$ events are also considered.

The tracking efficiency of charged pions has been investigated using control samples of $J/\psi \rightarrow p\bar{p}\pi^+\pi^-$ [29]. The difference in tracking efficiency between data and MC simulation is found to be 1% per track, which is taken as the uncertainty from the tracking efficiency.

TABLE I. Numbers used in the calculations of the product branching fractions and the upper limits, including the numbers of events, $N_{\text{obs}}(N_{\text{UL}})$, the detection efficiency, ε , and the product branching fractions, B . The world average values (PDG) are shown for comparison.

Decay mode	$N_{\text{obs}}(N_{\text{UL}})$	$\varepsilon(\%)$	B	PDG
$J/\psi \rightarrow \gamma\pi^0 \rightarrow 3\gamma$	1635 ± 54	29.03 ± 0.08	$(3.57 \pm 0.12 \pm 0.16) \times 10^{-5}$	$(3.45 \pm_{0.30}^{0.33}) \times 10^{-5}$
$J/\psi \rightarrow \gamma\eta \rightarrow 3\gamma$	18551 ± 158	27.18 ± 0.07	$(4.42 \pm 0.04 \pm 0.18) \times 10^{-4}$	$(4.35 \pm 0.14) \times 10^{-4}$
$J/\psi \rightarrow \gamma\eta' \rightarrow 3\gamma$	5057 ± 94	26.00 ± 0.08	$(1.26 \pm 0.02 \pm 0.05) \times 10^{-4}$	$(1.14 \pm 0.05) \times 10^{-4}$
$J/\psi \rightarrow \gamma\eta(1405) \rightarrow 3\gamma$	< 103	25.37 ± 0.09	$< 2.63 \times 10^{-6}$	–
$J/\psi \rightarrow \gamma\eta(1475) \rightarrow 3\gamma$	< 73	25.41 ± 0.11	$< 1.86 \times 10^{-6}$	–
$J/\psi \rightarrow \gamma\eta(1760) \rightarrow 3\gamma$	< 191	25.73 ± 0.12	$< 4.80 \times 10^{-6}$	–
$J/\psi \rightarrow \gamma X(1835) \rightarrow 3\gamma$	< 143	25.99 ± 0.11	$< 3.56 \times 10^{-6}$	–

TABLE II. Sources of relative systematic uncertainties and their contributions to the product branching fractions and upper limits (in %).

Source	π^0	η	η'	$\eta(1405)$	$\eta(1475)$	$\eta(1760)$	X(1835)
MDC tracking	2.0	2.0	2.0	2.0	2.0	2.0	2.0
Photon identification	3.0	3.0	3.0	3.0	3.0	3.0	3.0
4C kinematic fit	0.4	0.4	0.4	0.4	0.6	0.4	0.5
J/ψ mass window	0.2	0.2	0.2	0.2	0.2	0.2	0.2
Fit range	1.5	0.6	0.8	–	–	–	–
Background shape	1.3	1.0	0.8	–	–	–	–
Sideband region	0.9	0.4	0.6	–	–	–	–
MC statistics	0.3	0.3	0.3	0.4	0.4	0.5	0.4
$\psi(3686) \rightarrow \pi^+\pi^- J/\psi$	0.9	0.9	0.9	0.9	0.9	0.9	0.9
Number of $\psi(3686)$ events	0.6	0.6	0.6	0.6	0.6	0.6	0.6
Total	4.4	4.0	4.0	3.8	3.9	3.8	3.8

The photon detection efficiency is studied with a clean sample of $J/\psi \rightarrow \rho^0\pi^0$ [30]. The result shows that the difference of detection efficiency between data and MC simulation is 1% per photon.

The systematic uncertainties associated with the 4C kinematic fit are studied with the track helix parameter correction method, as described in Ref. [31]. In this analysis, we take the efficiencies with correction as the nominal values, and the differences with respect to those without corrections are taken as the systematic uncertainties associated with the 4C kinematic fit.

Due to the difference in the mass resolution between data and MC, the uncertainty related to the J/ψ mass window requirement is investigated by smearing the MC simulation in accordance with the signal shape of data. The change of the detection efficiency is assigned as the systematic uncertainty for the J/ψ mass window requirement.

To study the uncertainty from the fit range, the fit is repeated with different fit ranges, and the resultant largest differences in the signal yields are taken as the systematic uncertainties.

To estimate the uncertainty associated with the background shape, alternative fits with first-order or third-order Chebychev polynomial functions for the background are performed, and the maximum differences in signal yields with respect to the nominal values are taken as the systematic uncertainties.

The uncertainties from the J/ψ sideband region is estimated by using alternative sideband regions. The maximum differences in signal yields are taken as the uncertainties.

The uncertainty from the decay branching fractions of $\psi(3686) \rightarrow \pi^+\pi^- J/\psi$ is taken from the PDG [6], and the systematic uncertainty due to the number of $\psi(3686)$ events is determined to be 0.7% according to Ref. [17].

Table II summarizes the systematic uncertainties from all sources for each decay. The systematic uncertainties associated with the statistics of MC samples are also included. The total systematic uncertainty is obtained by adding all individual uncertainties in quadrature, assuming all sources to be independent.

V. RESULTS

The product branching fraction of $J/\psi \rightarrow \gamma P \rightarrow 3\gamma$ is calculated using

$$B(J/\psi \rightarrow \gamma P \rightarrow 3\gamma) = \frac{N_{\text{obs}} - N_{\text{bkg}}}{N_{\psi(3686)} \cdot B(\psi(3686) \rightarrow \pi^+\pi^- J/\psi) \cdot \varepsilon}, \quad (1)$$

where P represents the pseudoscalar meson, N_{obs} is the number of observed signal events determined from the fit to the $\gamma\gamma$ mass spectra, N_{bkg} is the number of peaking background events, $N_{\psi(3686)}$ is the total number of

$\psi(3686)$ events [17], ε is the MC-determined detection efficiency and $B(\psi(3686) \rightarrow \pi^+\pi^-J/\psi)$ is the branching fraction of $\psi(3686) \rightarrow \pi^+\pi^-J/\psi$ [6].

The product branching fractions of $J/\psi \rightarrow \gamma(\pi^0, \eta, \eta') \rightarrow 3\gamma$, are then determined to be $(3.57 \pm 0.12 \pm 0.16) \times 10^{-5}$, $(4.42 \pm 0.04 \pm 0.18) \times 10^{-4}$ and $(1.26 \pm 0.02 \pm 0.05) \times 10^{-4}$, respectively, as summarized in Table I. For comparison we also calculate the product branching fractions using the world average values of $B(J/\psi \rightarrow \gamma P)$ and $B(P \rightarrow \gamma\gamma)$ from the PDG [6], and the our measured branching fractions and the PDG branching fractions are summarized in Table I. The first two branching fractions are in good agreement with the world average values, which are dominated by the results from BESII [15] and CLEO [16], while the third one is slightly higher than the world average value, but consistent within two standard deviations.

To estimate the upper limits on product decay branching fractions for un-observed pseudoscalar mesons, the systematic uncertainties are taken into consideration by convolving the PDF of likelihood values in each decay with a Gaussian function $G(\mu, \sigma) = G(0, N\sigma_{\text{sys}})$, where N is the signal yield and σ_{sys} is the corresponding relative systematic uncertainty listed in Table II. The upper limits on the number of events and the branching fractions for $J/\psi \rightarrow \gamma[\eta(1405), \eta(1475), \eta(1760), X(1835)] \rightarrow 3\gamma$ at the 90% C.L. are listed in Table I. Using the branching fractions of $J/\psi \rightarrow \gamma\eta(1440) \rightarrow \gamma K\bar{K}\pi$ [32], $J/\psi \rightarrow \gamma\eta(1760) \rightarrow \gamma\omega\omega$ [8] and $J/\psi \rightarrow \gamma X(1835) \rightarrow \gamma\pi^+\pi^-\eta'$ [33] and their uncertainties, the upper limits at the 90% C.L. for the ratios of $\frac{B(\eta(1405) \rightarrow \gamma\gamma)}{B(\eta(1440) \rightarrow K\bar{K}\pi)}$, $\frac{B(\eta(1475) \rightarrow \gamma\gamma)}{B(\eta(1760) \rightarrow \omega\omega)}$ and $\frac{B(\eta(1760) \rightarrow \gamma\gamma)}{B(X(1835) \rightarrow \pi^+\pi^-\eta')}$ are determined to be 1.78×10^{-3} , 1.27×10^{-3} , 2.48×10^{-3} and 9.80×10^{-3} , respectively, and are reported for the first time in J/ψ decays.

ACKNOWLEDGMENTS

The BESIII collaboration thanks the staff of BEPCII and the IHEP computing center for their strong support. This work is supported in part by National Key Basic Research Program of China under Contract No. 2015CB856700; National Natural Science Foundation of China (NSFC) under Contracts Nos. 11565006, 11235011, 11335008, 11425524, 11625523, 11635010; the Chinese Academy of Sciences (CAS) Large-Scale Scientific Facility Program; the CAS Center for Excellence in Particle Physics (CCEPP); Joint Large-Scale Scientific Facility Funds of the NSFC and CAS under Contracts Nos. U1332201, U1232107, U1532257, U1532258; CAS under Contracts Nos. KJCX2-YW-N29, KJCX2-YW-N45, QYZDJ-SSW-SLH003; 100 Talents Program of CAS; National 1000 Talents Program of China; INPAC and Shanghai Key Laboratory for Particle Physics and Cosmology; German Research Foundation DFG under Contracts Nos. Collaborative Research Center CRC 1044, FOR 2359; Istituto Nazionale di Fisica Nucleare, Italy; Koninklijke Nederlandse Akademie van Wetenschappen (KNAW) under Contract No. 530-4CDP03; Ministry of Development of Turkey under Contract No. DPT2006K-120470; National Science and Technology fund; The Swedish Research Council; U. S. Department of Energy under Contracts Nos. DE-FG02-05ER41374, DE-SC-0010118, DE-SC-0010504, DE-SC-0012069; University of Groningen (RuG) and the Helmholtzzentrum fuer Schwerionenforschung GmbH (GSI), Darmstadt; WCU Program of National Research Foundation of Korea under Contract No. R32-2008-000-10155-0.

-
- [1] M. S. Chanowitz, Phys. Rev. Lett. **95**, 172001 (2005).
[2] D. L. Scharre *et al.*, Phys. Lett. B, **97**, 329 (1980).
[3] H. J. Behrend *et al.* (CELLO Collaboration), Z. Phys. C **42**, 367 (1989).
[4] G. S. Bali *et al.*, Phys. Lett. B **309**, 378 (1993).
[5] C. Morningstar and M. Peardon, Phys. Rev. D **60**, 034509 (1999).
[6] C. Patrignani *et al.* (Particle Data Group), Chin. Phys. C, **40**, 100001 (2016).
[7] P. R. Page and X. Q. Li, Eur. Phys. J. C **1**, 579 (1998).
[8] M. Ablikim *et al.* (BES Collaboration), Phys. Rev. D **73**, 112007 (2006).
[9] J. Z. Bai *et al.* (BES Collaboration), Phys. Lett. B **446**, 356 (1999).
[10] B. Loiseau and S. Wycech, Phys. Rev. C **72**, 011001 (2005).
[11] G. J. Ding, R. G. Ping, and M. L. Yan, Eur. Phys. J. A **28**, 351 (2006).
[12] B. A. Li, Phys. Rev. D **74**, 034019 (2006).
[13] Z. F. Sun, X. Liu, and Q. Zhao, Phys. Rev. D **83**, 114007 (2011).
[14] N. Kochelev and D. P. Min, Phys. Rev. D **72**, 097502 (2005).
[15] M. Ablikim *et al.* (BES Collaboration), Phys. Rev. D **73**, 052008 (2006).
[16] T. K. Pedlar *et al.* (CLEO Collaboration), Phys. Rev. D **79**, 111101(R) (2009).
[17] M. Ablikim *et al.* (BESIII Collaboration), Chin. Phys. C **37**, 063001 (2013); Chin. Phys. C **42**, 023001 (2018).
[18] M. Ablikim *et al.* (BESIII Collaboration), Nucl. Instrum. Meth. A **614**, 345 (2010).
[19] S. Agostinelli *et al.* (GEANT4 Collaboration), Nucl. Instrum. Meth. A **506**, 250 (2003).
[20] Z. Y. Deng *et al.*, Chin. Phys. C **30**, 371 (2006).
[21] S. Jadach, B. F. L. Ward and Z. Was, Comput. Phys. Commun. **130**, 260 (2000).
[22] S. Jadach, B. F. L. Ward and Z. Was, Phys. Rev. D **63**, 113009 (2001).
[23] R. G. Ping, Chinese Phys. C **32**, 599 (2008).
[24] D. J. Lange, Nucl. Instrum. Meth. A **462**, 152 (2001).

- [25] J. C. Chen, G. S. Huang, X. R. Qi, D. H. Zhang, and Y. S. Zhu, *Phys. Rev. D* **62**, 034003 (2000).
- [26] W. D. Li, H. M. Liu *et al.*, in proceeding of CHEP06, Mumbai, India, 2006 edited by Sunanda Banerjee (Tata Institute of Fundamental Reserach, Mumbai, (2006).
- [27] M. Ablikim *et al.* (BESIII Collaboration), *Phys. Rev. D* **92**, 052003 (2015).
- [28] J. H. Cheng *et al.*, *Nucl. Instrum. Meth. A* **827**, 165, (2016).
- [29] M. Ablikim *et al.* (BESIII Collaboration), *Phys. Rev. D* **83**, 112005 (2011).
- [30] M. Ablikim *et al.* (BESIII Collaboration), *Phys. Rev. D* **81**, 052005 (2010).
- [31] M. Ablikim *et al.* (BESIII Collaboration), *Phys. Rev. D* **87**, 012002 (2013).
- [32] J. Z. Bai *et al.* (BES Collaboration), *Phys. Lett. B* **25**, 476 (2000).
- [33] M. Ablikim *et al.* (BESIII Collaboration) *Phys. Rev. Lett.* **117**, 042002 (2016).